

Tuning the Hydrophobicity of a Mitochondria-Targeted NO Photodonor

Federica Sodano,^[a] Barbara Rolando,^[a] Francesca Spyraakis,^[a] Mariacristina Failla,^[b]
Loretta Lazzarato,^{*[a]} Elena Gazzano,^[c] Chiara Riganti,^{*[c]} Roberta Fruttero,^[a] Alberto Gasco,^[a]
and Salvatore Sortino^{*[b]}

A few compounds in which the nitric oxide (NO) photodonor *N*-[4-nitro-3-(trifluoromethyl)phenyl]propane-1,3-diamine is joined to the mitochondria-targeting alkyltriphenylphosphonium moiety via flexible spacers of variable length were synthesized. The lipophilicity of the products was evaluated by measuring their partition coefficients in *n*-octanol/water. The obtained values, markedly lower than those calculated, are consistent with the likely collapsed conformation assumed by the compounds in solution, as suggested by molecular dynamics simulations. The capacity of the compounds to release NO

under visible light irradiation was evaluated by measuring nitrite production by means of the Griess reaction. The accumulation of compounds in the mitochondria of human lung adenocarcinoma A549 cells was assessed by UPLC-MS. Interestingly, compound **13** [(9-((3-((4-nitro-3-(trifluoromethyl)phenyl)amino)propyl)amino)-9-oxononyl) triphenylphosphonium bromide] displayed both the highest accumulation value and high toxicity toward A549 cells upon irradiation-mediated NO release in mitochondria.

Introduction

Nitric oxide (NO) is an endogenous messenger ubiquitously produced by mammalian tissues and is involved in many physiological and pathophysiological processes.^[1] There is a significant amount of experimental evidence showing that low concentrations (nanomolar to picomolar levels) of NO encourage cancer growth, whereas high levels (micromolar) decrease cancer progression.^[2] The photogeneration of NO achieved by using suitable NO photodonors (NOPDs), has recently received a great deal of attention as a potential new anticancer therapy.^[3] Indeed, unlike classical NO donors,^[4] these light-activated precursors allow the action of NO to be confined within the irradiated area with high spatial precision, and its dosage to be controlled with great accuracy by tuning the duration and intensity of the irradiation.^[5] In contrast to traditional anticancer photodynamic therapy (PDT)^[6] based on the production of singlet oxygen (¹O₂),^[6] the so-called NO photodynamic therapy

(NOPDT)^[3] does not require O₂ availability to function. In particular, NOPDT may be useful in the treatment of hypoxic tumors which are not responsive to classical PDT.^[7]


Targeting mitochondria for cancer therapy is also currently generating great interest,^[8] and the role that NO plays in these organelles has received particular attention.^[9,10] NO may be formed in mitochondria by NOS (nitric oxide synthase) isoforms (eNOS, nNOS, iNOS), that are attached to the cytoplasmic face of the outer mitochondrial membrane and also, possibly, by a specific NOS isoform, referred to as mitochondrial NOS (mitNOS), located within these organelles. Low levels of NO upregulate cellular respiration and stimulate mitochondrial biogenesis. On the other hand, high levels of NO induce toxicity as this free radical directly binds and inhibits crucial mitochondrial enzymes, such as aconitase, a Fe-containing enzyme involved in the tricarboxylic acid cycle, and respiratory chain complexes containing iron and iron-sulfur centers, namely complexes I, III and IV. Furthermore, high NO levels produce reactive nitrogen (RNS) and oxygen (ROS) species and trigger mitochondrial apoptosis.^[9,10] The mitochondrial accumulation of NOPDs has therefore been proposed as an effective strategy for the design of new anticancer drugs. This approach has been created by linking the NOPDs to vectors that display high tropism for these organelles.^[11–15]

NOPD class nitro derivatives that bear appropriate substituents at the *o*- and *p*-positions have received particular attention. Under the action of violet light, these compounds undergo a nitro-to-nitrite rearrangement, followed by O–NO bond cleavage with consequent generation of NO and a phenoxy radical and, eventually, the formation of nontoxic phenol compounds.^[16,17] The flexibility of the *o*-CF₃ substituted *p*-nitroani-

[a] F. Sodano, Prof. B. Rolando, Prof. F. Spyraakis, Prof. L. Lazzarato, Prof. R. Fruttero, Prof. A. Gasco
Department of Science and Drug Technology, University of Torino, Via Pietro Giuria 9, 10125 Torino (Italy)
E-mail: loretta.lazzarato@unito.it

[b] M. Failla, Prof. S. Sortino
Laboratory of Photochemistry, Department of Drug Sciences, University of Catania, 95125 Catania (Italy)
E-mail: ssortino@unict.it

[c] Dr. E. Gazzano, Prof. C. Riganti
Department of Oncology, University of Torino, Via Santena 5/bis, 10126 Torino (Italy)
E-mail: chiara.riganti@unito.it

 Supporting information and the ORCID identification number(s) for the author(s) of this article can be found under:
<https://doi.org/10.1002/cmdc.201800088>.

line derivatives means that they are suited to this approach as their structures make their derivatization possible by simple synthetic methods. Rhodamine derivatives and triphenylphosphonium compounds have been used as vectors. The finished products are lipophilic cations with a largely delocalized positive charge that can enter mitochondria by binding the outer surface of the inner membrane. The high potential across this phospholipid bilayer ($\Delta\psi_m = 150\text{--}180\text{ mV}$), drives their passage to the inner surface where they are desorbed and accumulated in the mitochondrial matrix.^[18]

Although most solid tumors obtain their energy from aerobic glycolysis (Warburg effect), mitochondria still play a key role in tumor growth.^[19] Active mitochondria favor tumorigenesis, cell migration, metastasis^[20,21] and drug resistance.^[22,23] By contrast, impairing oxidative phosphorylation in mitochondria decreases cancer cell proliferation and invasion, and triggers apoptosis.^[19] Cancer cell mitochondria have higher transmembrane potentials than non-transformed cells.^[24] This feature indicates that mitochondrial activity is higher in tumor cells and this fact can be exploited to increase the selectivity of tumor cell killing by delivering drugs into the mitochondria.

As a further development of our work on NOPDs that are structurally related to *o*-(trifluoro)methyl-*p*-nitroaniline,^[15,25–27] we have designed a series of new compounds in which *N*-[4-nitro-3-(trifluoromethyl)phenyl]propane-1,3-diamine (**1**, Scheme 1), is linked through an amide bridge to alkyltriphenylphosphonium chains of variable length. This paper reports the synthesis, NO photorelease and partition coefficient ($\log P_{\text{oct/w}}$), of these compounds as well as those of the acetyl derivative of **1** (**2**, Scheme 1), used as suitable reference model. Furthermore, we analyze how lipophilicity affects the compounds' mitochondrial uptake in human lung adenocarcinoma A549 cells. Compound **13**, which shows the greatest tropism for mitochondria, was also investigated as regard its toxicity against

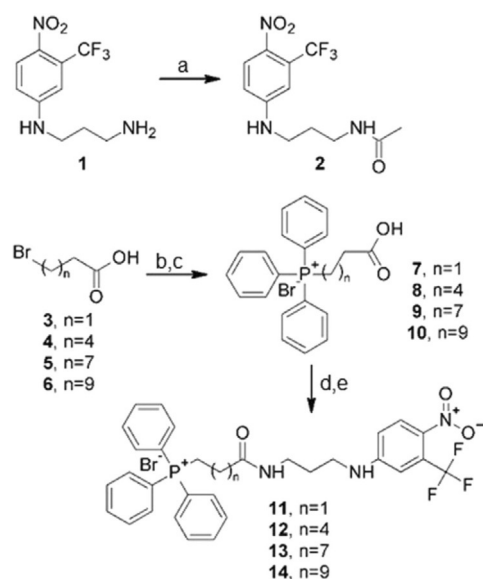
human lung adenocarcinoma cells, both in the dark and when irradiated with the violet light.

Results and Discussion

Synthesis and spectroscopic properties

The compounds studied in this work were obtained through the synthetic pathways reported in Scheme 1. The new NOPD **2** was prepared via the acetylation of **1**, synthesized according to literature,^[28] with acetic anhydride in dry CH_2Cl_2 , in the presence of triethylamine. The aliphatic carboxylic acids bearing the triphenylphosphonium moiety in the ω -position **7–10** were obtained from the reaction of related ω -bromo substituted acids **3–6** with triphenylphosphine (PPh_3), in either refluxing toluene or acetonitrile. Finally, target products **11–14** were synthesized via the coupling of **1** with the appropriate ω -triphenylphosphonium substituted acid in DMF and CH_2Cl_2 , in the presence of *N,N'*-dicyclohexylcarbodiimide (DCC), and *N*-hydroxysuccinimide (NHS).

The UV/Vis spectra, recorded in phosphate-buffered saline (PBS) solutions, of all the compounds are characterized, in the visible region, by the dominant absorption of the nitroaniline-chromophore centered at 402 nm (see Figure S1a in Supporting Information). The molar extinction coefficients ϵ follow the sequence **2–11** > **12** > **13** > **14**, which are different from observations made in methanol solution, where ϵ values are practically the same for all the products (see inset Figure S1 a, Supporting Information, as an example). This behavior is probably due to the formation of aggregates in PBS, which occurs to various extents. Irradiation of PBS solutions of all compounds with a 400 nm violet light-emitting diode (LED) at an irradiance of 7 mW cm^{-2} (the same irradiation conditions were used in all experiments described in this work) led to the typical bleaching of the visible absorption band, according to the release of NO .^[17] (see Figure S1 b, Supporting Information, as example).



Scheme 1. Synthesis of compounds **2**, **11**, **12**, **13** and **14**: a) $(\text{CH}_3\text{CO})_2\text{O}$, Et_3N , CH_2Cl_2 , 0°C ; b) PPh_3 , CH_3CN , Δ for compds **7** and **9**; c) PPh_3 , toluene, Δ for compds **8** and **10**; d) DCC, NHS, DMF; e) **1**, CH_2Cl_2 , DMF.

Lipophilicity

The partition coefficient ($\log P$), between *n*-octanol and PBS (pH 7.4), was chosen to describe the lipophilicity of the products. Measurements were carried out using the shake-flask technique, and results are reported in Table 1. The $\log P$ values range from 1.99 to 3.24. An attempt to calculate the $\log P$ of the products using the Hansch and Leo method on the CLOGP program (Bio-Loom for Windows, Version 1.5, BioByte), gave very high values which are unrealistic in nature. This molecular

Table 1. Partition coefficients ($\log P$), between *n*-octanol and PBS (pH 7.4), of compounds **2**, **11**, **12**, **13**, and **14**.

Compound	$\log P$ (\pm SD)
2	2.03(\pm 0.08)
11	1.99(\pm 0.05)
12	2.39(\pm 0.09)
13	2.78(\pm 0.08)
14	3.24(\pm 0.16)

descriptor has both additive and constitutive components. An analysis of the table shows that $\log P$ values increase, by 0.40 (11 to 12), 0.39 (12 to 13), and 0.46 (13 to 14), as we move from one compound to the next. This pattern is due to the presence of additional 3, 6, and 8 methylene units in 12, 13, 14, with respect to 11. If $f_{\text{CH}_2} = 0.66$ is taken as the CH_2 fragmental constant,^[29] one must conclude that the products are much less lipophilic than the simply additive nature of $\log P$ would provide for. It is most likely that a significant role in this $\log P$ decrement is played by the inter- and intramolecular hydrophobic interactions that form between the apolar parts of the molecules. Indeed, these interactions induce water molecules to strip off from the hydrophobic hydration shell (flickering cluster), and move to the bulk aqueous medium, leading to a subsequent decrease in molecular lipophilicity.^[29]

Compound conformation

To further investigate the conformations assumed by the compounds in solution, molecular dynamics (MD) simulations of 11, 12, 13, and 14 were performed. MD simulations were run using Gromacs 4.6.1 as implemented in the BiKi Life Science software suite (www.bikitech.com). All simulations were performed in water solution using the TIP3P water model (see the Experimental Section and Supporting Information for further details). An increase in methylene number generally leads the molecules to assume a more collapsed and globular conformation. These more ordered conformations are likely stabilized by hydrophobic interactions that form between the hydrophobic regions of the molecules; the nitroaniline, the triphenylphosphonium and the methylene units. In particular, the nitroaniline and phenyl rings that form the triphenylphosphonium moiety were observed to be in close contact to form π - π interactions (Figure 1).

To estimate the extent of ligand collapse in these molecules, the distances between the nitroaniline and triphenylphosphonium rings were calculated (see Figure S3 in Supporting Information). While compound 11 hardly folds back on itself at all, compounds 12, 13, and 14 spend a large part of the simulation time (20 ns), in collapsed globular forms. In particular, compound 13 shows the highest tendency to assume a globular structure, which is characterized by the presence of π - π contact. Different, but still collapsed, conformations are also assumed by the ligands when the nitroaniline folds back on the methylene unit (see Figure S2 in Supporting Information). Water molecules were displaced toward the bulk in all these forms, thus reducing the solvent accessible surface area of the ligands. As mentioned, this effect could, at least in part, explain the low $\log P$ increase observed upon the elongation of the methylene unit. It is interesting to note that the nitro group assumes an orthogonal orientation, which is indispensable requisite for the NO release mechanism.

NO photorelease in PBS solution

The capacity of 2 and 11–14 to release NO over 30 min of irradiation was evaluated at a concentration of 100 μM in 50 mM

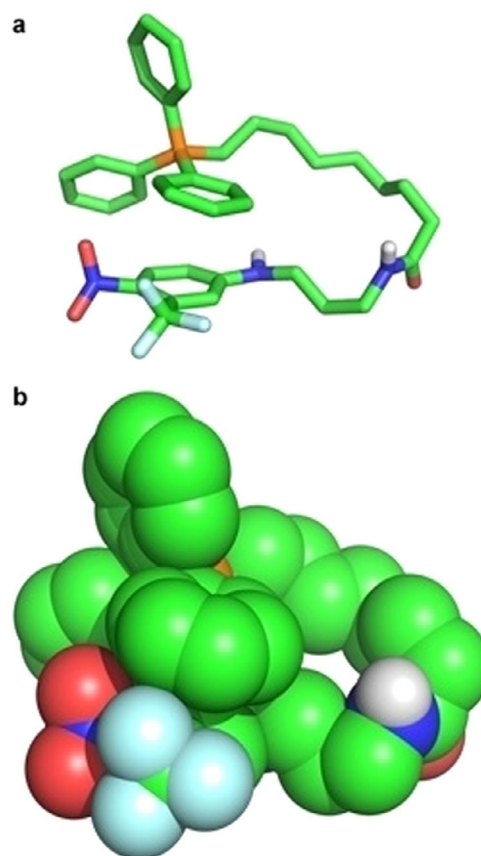


Figure 1. Compound 13 in the collapsed conformation, highlighting the close contact between the nitroaniline ring and one of the phenyl groups forming the triphenylphosphonium moiety. The ligand is shown in a) capped sticks and in b) spheres.

PBS (pH 7.4) using the experimental conditions described previously. Released NO was detected in the form of nitrite, its main degradation product, using the Griess reaction in aerobic aqueous solution. The results are summarized in Figure 2 and it is clear that the NO release of compounds is linearly correlated with time. All of the hybrid structures are better NOPDs than reference compound 2, and their performance can be graded as follows: 14–13 > 12 > 11 > 2.

The variety in the NO photoreleasing efficiency values observed for the five compounds can be, at first sight, quite surprising as the same NO photodonor moiety is present in all. However, we believe that the different conformations adopted by the investigated compounds play a key role in this respect. As summarized in the introduction, the NO release mechanism involves a nitro-to-nitrite rearrangement, followed by O–NO bond cleavage and the consequent generation of NO and a phenoxy radical, which is the key transient intermediate.^[16,17] In turn, the nitro-to-nitrite photorearrangement is triggered by the overlap between the p orbital of the nitro group oxygen and the π orbital of the phenyl ring.^[16,17] On these grounds, the collapsed conformation that is dominant in compounds 13 and 14 can, to some extent, not only encourage the above orbital overlap but also stabilize the intermediate phenoxy radical, which explains the fact that their NO photorelease efficiencies are higher than those of 2, 11 and 12.

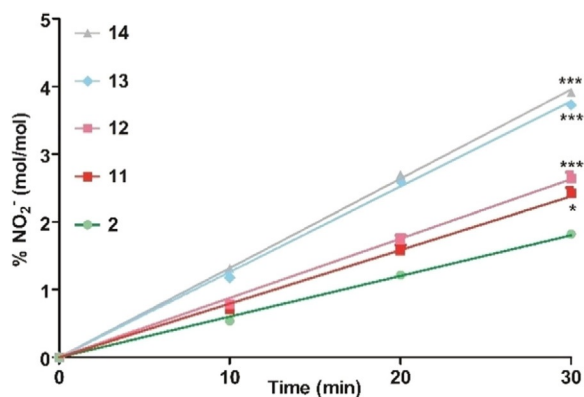


Figure 2. NO release profile upon LED irradiation ($\lambda = 400$ nm, 7 mW cm $^{-2}$), of 100 μ M solutions of **2** (green), **11** (red), **12** (fuchsia), **13** (light blue), and **14** (grey). NO release of compounds **11–14** vs. compound **2**: * $p < 0.05$; *** $p < 0.001$.

Accumulation in the mitochondria of human lung adenocarcinoma cells

The accumulation of **11–14** and reference **2** in mitochondria was assessed by incubating 5 μ M solutions of each compound with human lung adenocarcinoma A549 cells according to a previously described procedure.^[30] Briefly, the cytosolic and mitochondrial cellular fractions were separated after 4 h of incubation and the amounts of each compound in the two fractions was measured by UPLC–MS. The concentration found in the cytosol was 0.068 μ M for compound **2**, 0.103 μ M for **11**, 0.264 μ M for **12**, 2.701 μ M for **13** and 1.502 μ M for **14**. Mitochondrial accumulation was below the detection threshold for model compound **2**, 0.448 μ M for compound **11**, 1.105 μ M for **12**, 8.530 μ M for **13** and 4.042 μ M for **14**. The results are reported in Figure 3 and are normalized to mg of proteins in the cytosolic and mitochondrial fractions. Interestingly, while an accumulation increase occurs from **11** ($\log P = 1.99$), to **13** ($\log P = 2.78$), a decrease is observed from **13** to **14** ($\log P = 3.24$). As expected, the accumulation of reference compound **2** was not detectable. Consequently, compound **13** and reference compound **2**, which does not contain the alkyltriphenylphos-

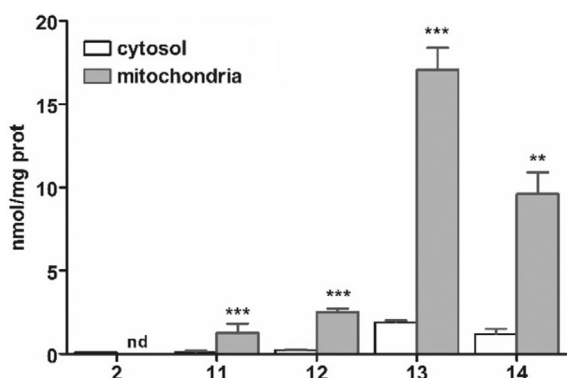


Figure 3. Mitochondrial and cytosolic accumulation of compounds **2** and **11–14**. Measurements were performed in triplicate and data are the mean \pm SEM; nd: not detectable. Mitochondrial vs. cytosolic accumulation: ** $p < 0.01$; *** $p < 0.001$.

phonium moiety, were chosen for antitumor property investigations.

NO photorelease by compounds **2** and **13** in lung adenocarcinoma cells

The NO photorelease of **2** and **13** in lung adenocarcinoma A549 cells, which had either been kept in the dark for 30 min or irradiated for the same time, was studied using the Griess reaction to detect nitrite. Concentrations of 5 μ M, considered nontoxic in the dark (see below), of the compounds were used in the experiments and the results are reported in Figure 4. While none of the compounds has the effect of increasing nitrite release in the dark relative to control cells, irradiation did induce this effect. In particular, compound **13** was a more effective NO donor than **2**, which is in line with results obtained in the cell-free experiments.

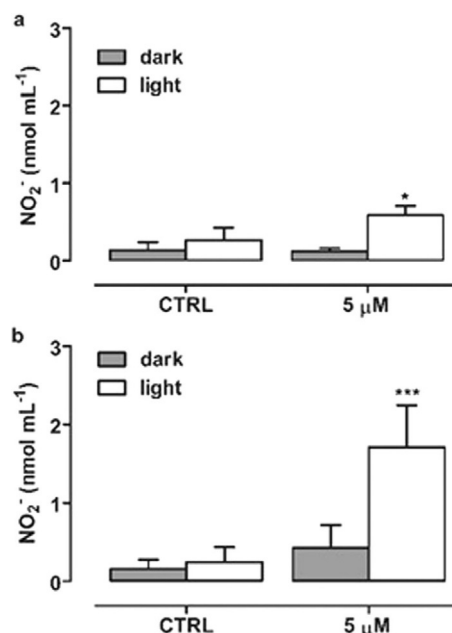


Figure 4. NO photorelease in A549 cells incubated with either model compound **2** (a) or **13** (b) and either maintained in the dark or irradiated ($\lambda = 400$ nm, 7 mW cm $^{-2}$), for 30 min. Measurements were performed in triplicate, and data are the mean \pm SD vs. untreated cells (CTRL): * $p < 0.05$; *** $p < 0.001$.

Cytotoxicity of compounds **2** and **13** against human lung adenocarcinoma cells

To evaluate the effect of mitochondrial accumulation on the toxicity of **13**, A549 cells were either left in the dark for 30 min or irradiated either in the presence of the compounds in a range of concentrations, or in their absence. Parallel experiments were carried out with reference **2** under the same conditions. Cytotoxicity was evaluated, 24 h after irradiation, by measuring the release of lactate dehydrogenase (LDH), which is sensitive to the loss of membrane integrity,^[31] and correlated well with the cell death. We have made use of the LDH release assay in our previous works on NO photodonors.^[15,27] The LDH

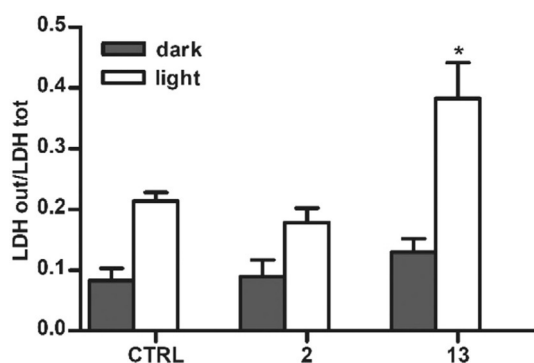


Figure 5. Cytotoxicity in A549 cells incubated with 5 μM solutions of compounds **2** and **13** and either maintained in the dark or irradiated ($\lambda = 400 \text{ nm}$, 7 mW cm^{-2}) for 30 min (light). Measurements were performed in triplicate, and data are the mean \pm SEM ($n = 3$) vs. untreated cells (CTRL): * $p < 0.05$.

assay was also performed here, as it is a sensitive index of irreversible cell damage leading to cell death, and to allow comparisons between the data obtained in the present work and in previous findings to be carried out.^[32] Figure 5 shows that the extent of cell death in both irradiated, untreated cells and in irradiated cells that had been treated with compound **2** is two times higher than that of non-irradiated cells. Moreover, the extent of cell death in irradiated cells that had been treated with compound **13** is four times that of not-irradiated cells, whether they were untreated or treated with either compound **2** or **13**. Reference **2** did not show any toxicity in the dark, unlike **13**, which was not significantly toxic up to a concentration of 5 μM and then showed enhanced toxicity with increasing concentration (data not shown). This is in keeping with the finding that phosphonium salts can display toxic activity toward cancer cell lines.^[33] When irradiated at 5 μM , **2** did not show any toxicity, unlike **13**, which was markedly more toxic, in keeping with its accumulation into mitochondria (Figure 5).

Conclusions

We have studied the influence of lipophilicity on the mitochondrial accumulation of a series of novel compounds obtained by linking alkyltriphenylphosphonium moieties to a nitroaniline-derivative NOPD. Interestingly, the dependence between the accumulation and $\log P$ of the products was roughly bilinear, showing a maximum for compound **13**. MD simulations demonstrated that methylene unit elongation generally leads the molecules to assume a more collapsed conformation, stabilized by the formation of hydrophobic interactions, which is probably responsible for the low estimated $\log P$. Compound **13** ($\log P = 2.78$), which shows the highest tendency to assume a globular structure, when irradiated triggered high toxicity at a 5 μM concentration, against A549 adenocarcinoma cell lines, unlike reference model **2**, which lacks the triphenylphosphonium moiety.

It is worth noting that the cytotoxicity induced by **13**, via NO release into mitochondria upon irradiation, falls in the low-micromolar range, which is similar to that of most antitumor chemotherapy drugs (e.g., anthracyclines, platinum derivatives,

gemcitabine). Our results may well facilitate the design of new efficient NOPDs which could potentially treat hypoxic tumors that are not responsive to classical PDT. Indeed, these compounds, unlike the classical photosensitizers for PDT, do not require $^1\text{O}_2$ production and therefore molecular oxygen availability in order to be active.

Experimental Section

Synthesis

All reactions involving air-sensitive reagents were performed under nitrogen in oven-dried glassware using the syringe-septum cap technique. All solvents were purified and degassed before use. Chromatographic separation was carried out under pressure on a Merck silica gel 60 using flash-column techniques. Reactions were monitored using thin-layer chromatography (TLC), carried out on 0.25 mm silica gel coated aluminum plates (Merck 60 F₂₅₄), using UV light (254 nm), a bromocresol green solution and a solution of diphenylamine in ethanol as the visualizing agents. Unless specified, all reagents were used as received without further purification. Dichloromethane was dried over P_2O_5 and freshly distilled under nitrogen prior to use. ^1H and ^{13}C NMR spectra were either recorded at room temperature on a Bruker Avance 300, at 300 and 75 MHz, or a JEOL ECZ-R 600, at 600 and 150 MHz, respectively, and calibrated using SiMe_4 as an internal reference. Chemical shifts (δ), are given in parts per million (ppm), and the coupling constants (J), in Hertz (Hz). The following abbreviations were used to designate multiplicities: s = singlet, d = doublet, dd = doublet of doublet, t = triplet, q = quartet, quint = quintet, m = multiplet, br = broad, bs = broad singlet. ESI spectra were recorded on a Micro-mass Quattro API micro (Waters Corporation, Milford, MA, USA), mass spectrometer. Data were processed using a MassLynx System (Waters). The purity of the final compounds ($\geq 95\%$), was determined by analytical HPLC analysis on a Merck LiChrospher C₁₈ end-capped column (250 \times 4.6 mm ID, 5 μm), using either $\text{CH}_3\text{CN}/\text{H}_2\text{O}$ or CH_3CN 0.1% TFA/ H_2O 0.1% TFA as the solvent. HPLC retention times (t_{R}), were obtained at flow rates of 1.0 mL min^{-1} and the column effluent was monitored using UV as the detector (DAD $\lambda = 226, 254, 400 \text{ nm}$). UV/Vis spectra absorption was recorded on a Varian Cary 50BIO UV/Vis spectrophotometer (Varian Australia Pty Ltd., Mulgrave, Australia), in air-equilibrated solutions, using quartz cells with a path length of 1 cm. Absorption spectral changes were monitored by irradiating the sample in a quartz cell (1 cm path length, 3 mL capacity), using a blue LED 10 W lamp as the light source and an irradiance of 7 mW cm^{-2} .

N-(3-((4-Nitro-3-(trifluoromethyl)phenyl)amino)propyl)acetamide (2): Acetic anhydride (1.21 mmol, 0.11 mL), and triethylamine (1.01 mmol, 0.14 mL), were added to a solution of **1** (1.01 mmol, 266 mg), in CH_2Cl_2 (10 mL), and stirred for 4 h at 0 $^\circ\text{C}$. H_2O (20 mL), was then added to the reaction mixture and the yellow solid **2** obtained was filtered and then dried under vacuum (160 mg, 53%); mp = 76.6–77.8 $^\circ\text{C}$. ^1H NMR (600 MHz, $[\text{D}_6]$ acetone): $\delta = 7.87$ (d, $J = 9.1 \text{ Hz}$, 1H), 6.90 (d, $J = 2.4 \text{ Hz}$, 1H), 6.71 (dd, $J = 9.1, 2.6 \text{ Hz}$, 1H), 3.22–3.07 (m, 4H), 1.70 (s, 3H), 1–69–1.63 ppm (m, 2H). ^{13}C NMR (150 MHz, $[\text{D}_6]$ acetone): $\delta = 170.6, 153.7, 135.6, 129.9, 126.3$ (q, $^2J_{\text{F}} = 32.8 \text{ Hz}$), 123.4 (q, $^1J_{\text{F}} = 272.6 \text{ Hz}$), 112.8, 111.7, 40.9, 37.0, 29.2, 22.6 ppm. ESI-MS $[M + \text{Na}]^+$: m/z 328.4. HPLC purity $\geq 95\%$ ($\text{CH}_3\text{CN}/\text{H}_2\text{O}$ 60:40 (v/v), flow = 1.0 mL min^{-1} , $t_{\text{R}} = 3.40 \text{ min}$) at 226, 254 and 400 nm.

General synthetic procedure for the preparation of aliphatic carboxylic acids bearing the triphenylphosphonium moiety in the

ω -position (7–10): A solution of the appropriate carboxylic acid **3–6** (1.0 equiv), and PPh_3 (2.0 equiv), was heated in either CH_3CN or toluene (20 mL), at reflux for 24 h. The reaction mixture was then purified as described below.

(2-Carboxyethyl)triphenylphosphonium bromide (7): The reaction was performed in CH_3CN . After 24 h, the solvent was removed under reduced pressure and the obtained residue was purified by flash chromatography using CH_2Cl_2 and then MeOH as the eluents, to give **7** as an orange oil (3.500 g, 84%). $^1\text{H NMR}$ (300 MHz, CDCl_3): δ = 7.89–7.60 (m, 15H), 6.14 (bs, 1H), 3.82–3.62 (m, 2H), 3.02–2.82 ppm (m, 2H). $^{13}\text{C NMR}$ (75 MHz, CDCl_3): δ = 171.8 (d, $^3J_{\text{p}} = 13.2$ Hz), 135.5 (d, $^4J_{\text{p}} = 3.0$ Hz), 133.7 (d, $^3J_{\text{p}} = 10.1$ Hz), 130.8 (d, $^2J_{\text{p}} = 12.6$ Hz), 117.6 (d, $^1J_{\text{p}} = 86.7$ Hz), 28.2 (d, $^2J_{\text{p}} = 2.5$ Hz), 19.0 ppm (d, $^1J_{\text{p}} = 54.7$ Hz). ESI-MS $[M]^+$: m/z 335.3.

(5-Carboxypentyl)triphenylphosphonium bromide (8): The reaction was performed in toluene. After 24 h, the obtained white solid **8** was filtered and then dried under vacuum. (2.00 g, 87%). $^1\text{H NMR}$ (300 MHz, CDCl_3): δ = 9.68 (bs, 1H), 7.95–7.58 (m, 15H), 3.5–3.26 (m, 2H), 2.40–2.19 (m, 2H), 1.71–1.55 ppm (m, 6H). $^{13}\text{C NMR}$ (75 MHz, CDCl_3): δ = 177.6, 135.4, 133.6 (d, $^3J_{\text{p}} = 10$ Hz), 130.7 (d, $^2J_{\text{p}} = 12.5$ Hz), 117.9 (d, $^1J_{\text{p}} = 86.2$ Hz), 33.8, 29.7 (d, $^2J_{\text{p}} = 16.2$ Hz), 24.0, 22.6 (d, $^1J_{\text{p}} = 51.4$ Hz), 22.2 ppm (d, $^3J_{\text{p}} = 3.6$ Hz). ESI-MS $[M]^+$: m/z 377.5.

(8-Carboxyoctyl)triphenylphosphonium bromide (9): The reaction was performed in CH_3CN . After 24 h, the solvent was removed under reduced pressure to give an oily residue. Purification by flash chromatography using $\text{CH}_2\text{Cl}_2/\text{MeOH}$ (96:4 to 85:15 v/v), as the eluent, gave **9** as an off-white semi-solid. (582 mg, 69%). $^1\text{H NMR}$ (600 MHz, $[\text{D}_6]\text{DMSO}$): δ = 7.96–7.73 (m, 15H), 3.67–3.49 (m, 2H), 3.39 (bs, 1H), 2.15 (t, $J = 7.4$ Hz, 2H), 1.58–1.39 (m, 6H), 1.31–1.14 ppm (m, 6H). $^{13}\text{C NMR}$ (150 MHz, $[\text{D}_6]\text{DMSO}$): δ = 174.6, 134.9 (d, $^4J_{\text{p}} = 3$ Hz), 133.6 (d, $^3J_{\text{p}} = 10$ Hz), 130.3 (d, $^2J_{\text{p}} = 12.5$ Hz), 118.6 (d, $^1J_{\text{p}} = 86$ Hz), 33.8, 30.7, 29.8 (d, $^2J_{\text{p}} = 16.5$ Hz), 28.5, 28.0, 24.5, 21.7 (d, $^3J_{\text{p}} = 4$ Hz), 20.1 ppm (d, $^1J_{\text{p}} = 50$ Hz). ESI-MS $[M]^+$: m/z 419.5.

(10-Carboxydecyl)triphenylphosphonium bromide (10): The reaction was performed in CH_3CN . After 24 h, the solvent was removed under reduced pressure to give an oily residue. Purification by flash chromatography using $\text{CH}_2\text{Cl}_2/\text{MeOH}$ (95:5 to 80:20, v/v), gave **10** as an off-white semi-solid. (2.200 g, 83%). $^1\text{H NMR}$ (300 MHz, CD_3OD): δ = 7.90–7.66 (m, 15H), 3.43–3.31 (m, 2H), 2.21 (t, $J = 7.4$ Hz, 2H), 1.70–1.44 (m, 6H), 1.36–1.16 ppm (m, 10H). $^{13}\text{C NMR}$ (75 MHz, CD_3OD): δ = 176.8, 135.3 (d, $^4J_{\text{p}} = 3.0$ Hz), 133.8 (d, $^3J_{\text{p}} = 10.0$ Hz), 130.5 (d, $^2J_{\text{p}} = 12.6$ Hz), 119.0 (d, $^1J_{\text{p}} = 86.3$ Hz), 34.0, 30.5 (d, $^2J_{\text{p}} = 16.2$ Hz), 29.4, 29.3, 29.2, 28.8, 25.1, 22.5 (d, $^3J_{\text{p}} = 4.4$ Hz), 21.6 ppm (d, $^1J_{\text{p}} = 51.0$ Hz). ESI-MS $[M]^+$: m/z 447.4.

General synthetic procedure for the preparation of target compounds (11–14): *N,N'*-dicyclohexylcarbodiimide (2.5 equiv), and *N*-hydroxysuccinimide (1.5 equiv) were added to a solution of the appropriate ω -triphenylphosphonium-substituted acid (**7–10**, 1 equiv), in dry DMF (40 mL), and the reaction mixture was stirred at room temperature for 4–12 h. When the reaction was completed (TLC), the solvent was removed under reduced pressure and the crude solid was triturated with cold CH_3CN and filtered under reduced pressure. The filtrate was concentrated to dryness and dissolved in dry $\text{CH}_2\text{Cl}_2/\text{DMF}$ (97:3, 31 mL). Compound **1** (1 equiv), was added to this solution and the mixture was stirred for 72 h at room temperature. The reaction mixture was then washed with H_2O (3 \times 20 mL), and brine (20 mL), dried over Na_2SO_4 and concentrated to dryness. Purification by flash chromatography, eluted with a different mixture of $\text{CH}_2\text{Cl}_2/\text{MeOH}$, gave target compounds as yellow foamy solids.

(3-((3-((4-Nitro-3-(trifluoromethyl)phenyl)amino)propyl)amino)-3-oxopropyl)triphenylphosphonium bromide (11): The carboxyl function activation reaction time was 4 h. Eluent: $\text{CH}_2\text{Cl}_2/\text{MeOH}$, 98:2 to 95:5, v/v. The target compound **11** was as a foamy yellow solid (yellow solid^[13]) (923 mg, 58%). $^1\text{H NMR}$ (300 MHz, $[\text{D}_6]\text{DMSO}$): δ = 8.03 (d, $J = 9.1$ Hz, 1H), 7.92–7.63 (m, 15H), 7.03–6.96 (m, 1H), 6.75 (dd, $J = 9.2, 2.2$ Hz, 1H), 3.82–3.65 (m, 2H), 3.15–2.97 (m, 4H), 2.06–2.00 (m, 2H), 1.65–1.51 ppm (m, 2H). $^{13}\text{C NMR}$ (75 MHz, $[\text{D}_6]\text{DMSO}$): δ = 168.7 (d, $^3J_{\text{p}} = 15.0$ Hz), 153.2, 135.0, 133.7 (d, $^3J_{\text{p}} = 10.2$ Hz), 133.5, 130.3 (d, $^2J_{\text{p}} = 12.5$ Hz), 129.9, 126.4 (q, $^1J_{\text{F}} = 248.9$ Hz), 118.4 (d, $^1J_{\text{p}} = 86.3$ Hz), 36.6, 30.8, 27.9, 27.5, 16.9 ppm (d, $^1J_{\text{p}} = 53.4$ Hz). ESI-MS $[M]^+$: m/z 580.3. HPLC purity = 96% (CH_3CN 0.1% TFA/ H_2O 0.1% TFA 65:35 (v/v), flow = 1.0 mL min⁻¹, t_{R} = 6.4 min), at 226, 254 and 400 nm.

(6-((3-((4-Nitro-3-(trifluoromethyl)phenyl)amino)propyl)amino)-6-oxohexyl)triphenylphosphonium bromide (12): The carboxyl function activation reaction time was 4 h. Eluent: $\text{CH}_2\text{Cl}_2/\text{MeOH}$, 98:2 to 95:5, v/v. The target compound **12** was as a foamy yellow solid (489 mg, 70%). $^1\text{H NMR}$ (600 MHz, $[\text{D}_6]\text{DMSO}$): δ = 8.01 (d, $J = 9.1$ Hz, 1H), 7.78–7.67 (m, 15H), 7.02–6.96 (m, 1H), 6.77–6.74 (m, 1H), 3.55–3.47 (m, 2H), 3.12 (dd, $J = 12.7, 6.8$ Hz, 2H), 3.05 (q, $J = 6.7, 2$ Hz), 1.98 (t, $J = 7.2$ Hz, 2H), 1.61 (quin, $J = 6.9$ Hz, 2H), 1.49–1.34 ppm (m, 6H). $^{13}\text{C NMR}$ (150 MHz, $[\text{D}_6]\text{DMSO}$): δ = 172.0, 153.2, 135.0 (d, $^4J_{\text{p}} = 3.0$ Hz), 133.6 (d, $^3J_{\text{p}} = 10.1$ Hz), 133.5, 130.3 (d, $^2J_{\text{p}} = 12.6$ Hz), 122.6 (q, $^1J_{\text{F}} = 272.7$ Hz), 118.6 (d, $^1J_{\text{p}} = 85.5$), 36.2, 35.1, 30.8, 29.6 (d, $^2J_{\text{p}} = 16.3$ Hz), 28.2, 24.5, 21.7 (d, $^3J_{\text{p}} = 3.2$ Hz), 20.2 ppm (d, $^1J_{\text{p}} = 49.8$ Hz). ESI-MS $[M]^+$: m/z 622.3. HPLC purity = 97% (CH_3CN 0.1% TFA/ H_2O 0.1% TFA 65:35 (v/v), flow = 1.0 mL min⁻¹, t_{R} = 7.4 min), at 226, 254 and 400 nm.

(9-((3-((4-Nitro-3-(trifluoromethyl)phenyl)amino)propyl)amino)-9-oxononyl)triphenylphosphonium bromide (13): The carboxyl function activation reaction time was 6 hours. Eluent: $\text{CH}_2\text{Cl}_2/\text{MeOH}$, 98:2 to 85:15, v/v. The target compound **13** was as a foamy yellow solid (340 mg, 79%). $^1\text{H NMR}$ (300 MHz, CD_3OD): δ = 7.95 (d, $J = 9.2$ Hz, 1H), 7.89–7.66 (m, 15H), 6.93 (d, $J = 2.2$ Hz, 1H), 6.72 (dd, $J = 9.2, 2.5$ Hz, 1H), 3.44–3.29 (m, 2H), 3.29–3.16 (m, 4H), 2.12 (t, $J = 7.4$ Hz, 2H), 1.87–1.71 (m, 2H), 1.69–1.42 (m, 6H), 1.35–1.15 ppm (m, 6H). $^{13}\text{C NMR}$ (75 MHz, CD_3OD): δ = 174.9, 154.4, 136.8 (d, $^4J_{\text{p}} = 3.0$ Hz), 134.8 (d, $^3J_{\text{p}} = 10.0$ Hz), 131.5 (d, $^2J_{\text{p}} = 12.6$ Hz), 130.4, 127.3 (q, $^2J_{\text{F}} = 32.8$ Hz), 124.0 (q, $^1J_{\text{F}} = 273.0$ Hz), 119.9 (d, $^1J_{\text{p}} = 86.3$ Hz), 112.9, 112.1, 41.4, 37.4 (d, $^1J_{\text{p}} = 57.6$ Hz), 31.5 (d, $^2J_{\text{p}} = 16.3$ Hz), 30.1, 29.7, 29.4, 26.9, 23.5 (d, $^3J_{\text{p}} = 4.4$ Hz), 22.9, 22.3 ppm. ESI-MS $[M]^+$: m/z 664.5. HPLC purity = 100% (CH_3CN 0.1% TFA/ H_2O 0.1% TFA 65/35 (v/v), flow = 1.0 mL min⁻¹, t_{R} = 9.7 min), at 226, 254 and 400 nm.

(11-((3-((4-Nitro-3-(trifluoromethyl)phenyl)amino)propyl)amino)-11-oxoundecyl)triphenylphosphonium bromide (14): The carboxyl function activation reaction time was 12 h. Eluent: $\text{CH}_2\text{Cl}_2/\text{MeOH}$, 95:5 to 90:10, v/v. The target compound **14** was as a foamy yellow solid (415 mg, 40%). $^1\text{H NMR}$ (300 MHz, CDCl_3): δ = 7.90 (d, $J = 9.1$ Hz, 1H), 7.85–7.64 (m, 15H), 7.01–6.95 (m, 1H), 6.78–6.68 (m, 1H), 3.39–3.28 (m, 6H), 2.27 (t, $J = 7.5$ Hz, 2H), 1.87–1.76 (m, 2H), 1.72–1.47 (m, 6H), 1.35–1.10 ppm (m, 10H). $^{13}\text{C NMR}$ (75 MHz, CDCl_3): δ = 174.6, 169.4, 153.0, 135.5 (d, $^4J_{\text{p}} = 3.0$ Hz), 134.3, 133.6 (d, $^3J_{\text{p}} = 9.9$ Hz), 130.7 (d, $^2J_{\text{p}} = 12.5$ Hz), 129.5, 126.6 (q, $^2J_{\text{F}} = 32.9$ Hz), 122.7 (q, $^1J_{\text{F}} = 272.2$ Hz), 118.1 (d, $^1J_{\text{p}} = 86.1$ Hz), 39.9, 36.5, 36.3, 30.3 (d, $^2J_{\text{p}} = 15.9$ Hz), 28.9, 28.8, 28.6 (d, $^3J_{\text{p}} = 3.2$ Hz), 28.3, 27.1, 25.7, 22.9 (d, $^1J_{\text{p}} = 44.6$ Hz), 22.5 ppm. ESI-MS $[M]^+$: m/z 692.4. HPLC purity = 95% (CH_3CN 0.1% TFA/ H_2O 0.1% TFA 65:35 (v/v), flow = 1.0 mL min⁻¹, t_{R} = 13.8 min), at 226, 254 and 400 nm.

Determination of lipophilicity descriptor ($\log P$)

The partition coefficients ($\log P$), of the target compounds between *n*-octanol and PBS (pH 7.4), were obtained using the shake-flask technique at room temperature. In the shake-flask experiments, 50 mM PBS (pH 7.4), was used as the aqueous phase and ionic strength was adjusted to 0.15 M using KCl. The organic (*n*-octanol), and aqueous phases were mutually saturated by shaking for 4 h. The compounds were solubilized in the buffered aqueous phase at concentrations of either 0.1 mM or 0.05 mM, depending on their solubility, and appropriate amounts of *n*-octanol were added. The two phases were shaken for about 20 min, by which time the partitioning equilibrium of the solutes had been reached, and then centrifuged (10000 rpm, 10 min). The concentration of the solutes was measured in the aqueous phase using UV spectrophotometer (UV-2501PC, Shimadzu). Each $\log P$ value is an average of at least six measurements. All the experiments were performed while avoiding exposure to light.

Molecular dynamics

The ligands were parameterized using the ab initio RESP-charge-fitting methodology, as implemented in the BiKi Life Science software suite (www.bikitech.com). MD simulation setup was performed using BiKi. Gromacs 4.6.1 was used to run MD simulations.^[34] The water model used was TIP3P. The solvated system was preliminarily minimized by 5000 steps of steepest descent. As in the subsequent equilibration, the integration step was equal to 1 fs. The Verlet cut-off scheme, the Bussi–Parrinello thermostat^[35] LINCS for the constraints (all bonds), and the particle mesh Ewald for electrostatics, with a short-range cutoff of 11 Å, were used. The system was equilibrated in four subsequent steps: 100 ps in the NVT ensemble at 100 K, 100 ps in the NVT ensemble at 200 K, 100 ps in the NVT ensemble at 300 K and a 1 ns long NPT simulation in order to reach the pressure equilibrium condition. No restraint was applied. The production run was carried out in the NVT ensemble at 300 K without any restraint for 20 ns. Two replicas were simulated for each ligand upon velocity reassignment.

NO photorelease

NO release was evaluated, as nitrite formed, using the Griess reaction; 5 mL of 100 μ M solutions of compounds **2**, **11**, **12**, **13** and **14** in 50 mM pH 7.4 PBS solution, and 1% DMSO were irradiated using a violet LED 10 W lamp. An irradiance of 7 mW cm⁻² was measured with an HD2302.0 Delta Ohm light meter equipped with a Delta Ohm LP471RAD light probe. The presence of nitrite was determined at regular time intervals using the Griess assay; 1.0 mL of the reaction mixture was treated with 250 μ L of Griess reagent (4% w/v sulfanilamide, 0.2% w/v *N*-naphthylethylenediamine dihydrochloride, 1.47 M phosphoric acid). After 10 min at room temperature, the reaction mixture was analyzed using a UV spectrophotometer Shimadzu UV-2501PC and calibration curves obtained with standard solutions of sodium nitrite at 0.5 μ M to 50 μ M ($r^2 > 0.99$). The nitrite yield was expressed as percentage of NO₂⁻ (mol mol⁻¹, relative to the initial compound concentration) \pm SEM.

Biological experiments

The culture media were obtained from Invitrogen Life Technologies (Carlsbad, CA, USA), while plasticware for cell cultures was obtained from Falcon (Becton Dickinson, Franklin Lakes, NJ, USA). The protein content of cell monolayers and lysates was assessed using

the BCA kit from Sigma Chemical Co. (St. Louis, MO, USA). Unless otherwise specified, all the reagents were obtained from Sigma Chemical Co. The test compounds were dissolved in dimethyl sulfoxide (DMSO), and then diluted in culture medium to achieve the final concentration. The concentration of DMSO in the culture medium in all the experiments was lower than 0.1%, a concentration that did not affect cell viability (data not shown).

Cells: Human lung adenocarcinoma A549 cells, provided by Istituto Zooprofilattico Sperimentale "Bruno Ubertyni" (Brescia, Italy), were cultured in Ham's F12 medium supplemented with 10% fetal bovine serum and 1% penicillin–streptomycin. Cell cultures were kept in a humidified atmosphere at 37 °C and 5% CO₂. When indicated, cells were placed in Ham's F12 medium without phenol red and exposed for 30 min to the light emitted by a 400 nm, 10 W violet LED, using an irradiance of 7 mW cm⁻². Non-irradiated cells were kept in a dark room for 30 minutes in Ham's F12 medium without phenol red at room temperature. After this period, cells were left for 19.5 h in the incubator before the experimental procedures described below were carried out.

Mitochondria accumulation: For the mitochondrial accumulation experiments, A549 cells were incubated for 4 h with the compounds and the mitochondria were then extracted, as described earlier.^[30] A 50 μ L aliquot was sonicated and used for protein content measurements and Western blotting. The remainder was stored at -80 °C until use. 10 μ g of each sonicated sample was subjected to SDS-PAGE and probed with an anti-VDAC/porin antibody in order to confirm the presence of mitochondrial proteins in the extracts (Abcam; data not shown). The quantity of compounds (**2**, **11–14**), in the mitochondrial and cytosolic fractions was measured using an Acquity Ultra Performance LC (Waters Corporation Milford MA, USA), equipped with BSM, SM, CM and PDA detectors. The analytical column was a Zorbax Eclipse XDB-C₁₈, 150 \times 4.6 mm \times 5 μ m. The mobile phase consisted of CH₃CN 0.1% HCOOH/H₂O 0.1% HCOOH 70/30 v/v for compound **2**, and CH₃CN 0.1% HCOOH/H₂O 0.1% HCOOH 60:40 v/v for compounds **11–14**. UPLC retention time (t_R), was obtained at flow rates of 0.5 mL min⁻¹ and the column effluent was monitored using a Micromass Quattro micro API Esci with multi-mode ionization enabled, as the detector. The molecular ions $[M+H]^+$ for **2** and $[M]^+$ for **11–14** were used for the quantitative measurements of the analyte. MS conditions were as follows: drying gas (nitrogen), heated at 350 °C at a flow rate of 800 L h⁻¹; nebulizer gas (nitrogen), at 80 L h⁻¹; capillary voltage in positive mode at 3000 V; fragmentor voltage at 30 V. The values obtained from the integration of compound peaks were interpolated into calibration curves obtained using standard solutions at 0.1 μ M to 5 μ M ($r^2 = 0.996$). The quantity of compounds in the mitochondrial and cytosolic fractions was expressed as nmol/(mg protein).

NO photorelease in cells: Cells were incubated and irradiated as described in the Cells section above. 1 mL of cell supernatant was then collected and centrifuged for 10 minutes at 13000 g. The presence of nitrite in the supernatants was determined using the Griess assay; 0.5 mL of the reaction mixture was treated with 125 mL of the Griess reagent (4% w/v sulfanilamide, 0.2% w/v *N*-naphthylethylenediamine dihydrochloride, 1.47 mM phosphoric acid), after 10 min at room temperature, the sample was analyzed by RP-HPLC in order to detect the azo dye. HPLC analyses were performed using a HP 1200 chromatograph system (Agilent Technologies, Palo Alto, CA, USA), equipped with a quaternary pump (model G1311A), a membrane degasser (G1322A), and a multiple wavelength UV detector (MWD, model G1365D), integrated into the system. Data analyses were performed using a HP ChemStation

system (Agilent Technologies). Samples were eluted on a HyPURITY Elite C₁₈ column (250 × 4.6 mm, 5 mm, Hypersil, ThermoQuest Corporation, UK). The injection volume was 20 μL (Rheodyne, Cotati, CA, USA). The mobile phase consisted of CH₃CN 0.1% TFA (solvent A), and H₂O 0.1% TFA (solvent B), at a flow rate of 1.0 mL min⁻¹ with gradient conditions: 50% A up to 4 min, from 50 to 90% A between 4 and 8 min, 90% A between 8 and 12 min, and from 90 to 50% A between 12 and 15 min. The column effluent was monitored at 540 nm, referenced against an 800 nm wavelength. Data analysis was performed using Agilent ChemStation. The values obtained from the integration of the azo dye peak were interpolated into a calibration curve obtained using standard solutions of sodium nitrite from 0.5 μM to 50 μM ($r^2 = 0.996$). The nitrite yield was expressed as percent NO₂⁻ (mol mol⁻¹, relative to the initial compound concentration) ± SEM.

Cytotoxicity: The cytotoxic effect of the compounds was measured as the leakage of lactate dehydrogenase (LDH), activity into the extracellular medium using a Synergy HT microplate reader (Bio-Tek Instruments, Winooski, VT, USA), as previously described.^[31] Both intracellular and extracellular LDH were measured and then extracellular LDH activity (LDH out), was calculated as a percentage of the total (intracellular + extracellular), LDH activity (LDH tot), in the dish.

Statistical analysis: All data are provided as means ± SEM. Results were analyzed using one-way analysis of variance (ANOVA), and Turkey's test (software: SPSS 21.0 for Windows, SPSS Inc., Chicago, IL, USA); $p < 0.05$ was considered significant.

Acknowledgements

We thank AIRC, Project IG-19859 and the University of Turin (Ricerca Locale ex 60%) for financial support. We thank the Centro di Competenza sul Calcolo Scientifico (C3S) at the University of Turin (c3s.unito.it) for providing computational time and resources.

Conflict of interest

The authors declare no conflict of interest.

Keywords: mitochondria · nitric oxide · phosphonium salts · photoactivation · targeted therapy

- [1] a) J. F. Kerwin, Jr., J. R. Lancaster, P. L. Feldman, *J. Med. Chem.* **1995**, *38*, 4343–4362; b) J. F. Kerwin, Jr., M. Heller, *Med. Res. Rev.* **1994**, *14*, 23–74.
- [2] a) Z. Huang, J. Fu, Y. Zhang, *J. Med. Chem.* **2017**, *60*, 7617–7635; b) Q. Ma, Z. Wang, M. Zhang, H. Hu, J. Li, D. Zhang, K. Guo, H. Sha, *Curr. Pharm. Des.* **2010**, *16*, 392–410.
- [3] A. D. Ostrowski, P. C. Ford, *Dalton Trans.* **2009**, *48*, 10660–10669.
- [4] S. Huerta, B. Chilka, B. Bonavida, *J. Oncol.* **2008**, *33*, 909–927.
- [5] For example, see: a) S. Sortino, *Chem. Soc. Rev.* **2010**, *39*, 2903; b) P. C. Ford, *Acc. Chem. Res.* **2008**, *41*, 190; c) N. L. Fry, P. K. Mascharak, *Acc. Chem. Res.* **2011**, *44*, 289; d) P. C. Ford, *Nitric Oxide* **2013**, *34*, 56; e) A. Fraix, S. Sortino, *Chem. Asian J.* **2015**, *10*, 1116; f) A. Fraix, N. Marino, S. Sortino, *Top. Curr. Chem.* **2016**, *370*, 225.
- [6] P. Agostinis, K. Berg, K. A. Cengel, T. H. Foster, A. W. Girotti, S. O. Gollnick, S. M. Hahn, M. R. Hamblin, A. Juzeniene, D. Kessel, M. Korblick, J. Moan, P. Mroz, D. Nowis, J. Piette, B. C. Wilson, J. Golab, *CA Cancer J. Clin.* **2011**, *61*, 250–281.

- [7] C. Fowley, A. P. McHale, B. McCaughan, A. Fraix, S. Sortino, J. F. Callan, *Chem. Commun.* **2015**, *51*, 81–84.
- [8] a) S. Fulda, L. Galluzzi, G. Kroemer, *Nat. Rev.* **2010**, *9*, 447–463; b) M. C. Frantz, P. Wipf, *Environ. Mol. Mutagen.* **2010**, *51*, 462–475; c) S. Wen, D. Zhu, P. Huang, *Future Med. Chem.* **2013**, *5*, 53–67.
- [9] S. Moncada, J. D. Erusalimsky, *Nat. Rev. Mol. Cell. Biol.* **2002**, *3*, 214–220.
- [10] G. C. Brown, *Front. Biosci.* **2007**, *12*, 1024–1033.
- [11] T. Horinouchi, H. Nakagawa, T. Suzuki, K. Fukuhara, N. Miyata, *Bioorg. Med. Chem. Lett.* **2011**, *21*, 2000–2002.
- [12] T. Horinouchi, H. Nakagawa, T. Suzuki, K. Fukuhara, N. Miyata, *Chem. Eur. J.* **2011**, *17*, 4809–4813.
- [13] J. Xu, F. Zeng, H. Wu, C. Hu, C. Yu, S. Wu, *Small* **2014**, *10*, 3750–3760.
- [14] J. Xu, F. Zeng, H. Wu, S. Wu, *J. Mater. Chem. B* **2015**, *3*, 4904–4912.
- [15] F. Sodano, E. Gazzano, A. Fraix, B. Rolando, L. Lazzarato, M. Russo, M. Blangetti, C. Riganti, R. Fruttero, A. Gasco, S. Sortino, *ChemMedChem* **2018**, *13*, 87–96.
- [16] a) T. Suzuki, O. Nagae, Y. Kato, H. Nakagawa, K. Fukuhara, N. Miyata, *J. Am. Chem. Soc.* **2005**, *127*, 11720–11726; b) K. Kitamura, N. Ieda, K. Hishikaw, T. Suzuki, N. Miyata, K. Fukuhara, H. Nakagawa, *Med. Chem. Lett.* **2014**, *24*, 5660–5662.
- [17] a) E. B. Caruso, S. Petralia, S. Conoci, S. Giuffrida, S. Sortino, *J. Am. Chem. Soc.* **2007**, *129*, 480–481; b) S. Conoci, S. Petralia, S. Sortino (STMiroelectronics SRL), Eur. Pat. No. EP2051935A1, US20090191284, **2006**.
- [18] J. Zielonka, J. Joseph, A. Sikora, M. Hardy, O. Ouari, J. Vasquez-Vivar, G. Cheng, M. Lopez, B. Kalyanaraman, *Chem. Rev.* **2017**, *117*, 10043–10120.
- [19] A. P. Trotta, J. E. Chipuk, *Cell. Mol. Life Sci.* **2017**, *74*, 1999–2017.
- [20] M. C. Caino, J. C. Ghosh, Y. C. Chae, V. Vaira, D. B. Rivadeneira, A. Favarsani, P. Rampini, A. V. Kossenkov, K. M. Aird, R. Zhang, M. R. Webster, A. T. Weeraratna, S. Bosari, L. R. Languino, D. C. Altieri, *Proc. Natl. Acad. Sci. USA* **2015**, *112*, 8638–8643.
- [21] L. García-Ledo, C. Nuevo-Tapioles, C. Cuevas-Martín, I. Martínez-Reyes, B. Soldevilla, L. González-Llorente, J. M. Cuezva, *Front. Oncol.* **2017**, *7*, 69.
- [22] C. Riganti, E. Gazzano, G. R. Gulino, M. Volante, D. Ghigo, J. Kopecka, *Cancer Lett.* **2015**, *360*, 219–226.
- [23] I. Buondonno, E. Gazzano, S. R. Jean, V. Audrito, J. Kopecka, M. Fanelli, I. C. Salaroglio, C. Costamagna, I. Roato, E. Mungo, C. M. Hattinger, S. Deaglio, S. O. Kelley, M. Serra, C. Riganti, *Mol. Cancer Ther.* **2016**, *15*, 2640–2652.
- [24] J. Modica-Napolitano, J. Aprille, *Adv. Drug Delivery Rev.* **2001**, *49*, 63–70.
- [25] A. Fraix, S. Guglielmo, V. Cardile, A. C. E. Graziano, R. Gref, B. Rolando, R. Fruttero, A. Gasco, S. Sortino, *RSC Adv.* **2014**, *4*, 44827–44836.
- [26] A. Fraix, M. Blangetti, S. Guglielmo, L. Lazzarato, N. Marino, V. Cardile, A. C. E. Graziano, I. Manet, R. Fruttero, A. Gasco, S. Sortino, *ChemMedChem* **2016**, *11*, 1371–1379.
- [27] K. Chegaev, A. Fraix, E. Gazzano, G. E. F. Abd-Ellatef, M. Blangetti, B. Rolando, S. Conoci, C. Riganti, R. Fruttero, A. Gasco, S. Sortino, *ACS Med. Chem. Lett.* **2017**, *8*, 361–365.
- [28] F. L. Callari, S. Sortino, *Chem. Commun.* **2008**, 1971–1973.
- [29] C. Hansch, A. J. Leo in *ACS Professional Reference Book*, American Chemical Society, Washington DC, **1995**.
- [30] I. Campia, C. Lussiana, G. Pescarmona, D. Ghigo, A. Bosia, C. Riganti, *Br. J. Pharmacol.* **2009**, *158*, 1777–1786.
- [31] E. Aldieri, I. Fenoglio, F. Cesano, E. Gazzano, G. Gulino, A. Scarano, D. Atanasio, G. Mazzucco, D. Ghigo, B. Fubini, *J. Toxicol. Environ. Health Part A* **2013**, *76*, 1056–1071.
- [32] E. Gazzano, B. Rolando, K. Chegaev, I. C. Salaroglio, J. Kopecka, I. Pedrini, S. Saponara, M. Sorge, I. Buondonno, B. Stella, A. Marengo, M. Valoti, M. Brancaccio, R. Fruttero, A. Gasco, S. Arpicco, C. Riganti, *J. Controlled Release* **2018**, *270*, 37–52.
- [33] B. Bachowska, J. Kazmierczak-Baranska, M. Cieslak, B. Nawrot, D. Szczesna, J. Skalik, P. Balczewski, *ChemistryOpen* **2012**, *1*, 33–38.
- [34] B. Hess, C. Kutzner, D. Van der Spoel, E. Lindahl, *J. Chem. Theory Comput.* **2008**, *4*, 435–447.
- [35] G. Bussi, D. Donadio, M. Parrinello, *J. Chem. Phys.* **2007**, *126*, 014101.

Manuscript received: February 9, 2018

Revised manuscript received: April 3, 2018

Accepted manuscript online: April 6, 2018

Version of record online: May 8, 2018